Development of an atmospheric correction algorithm for hyperspectral remote sensing of ocean color from space

Bo-Cai Gao[1], Marcos J. Montes[1], Ziauddin Ahmad[2], and Curtiss O. Davis[1]
[1]Remote Sensing Division, Code 7212, Naval Research Laboratory, Washington, DC 20375
[2]Science and Data Systems, Inc., 16509 Copperstrip Lane, Silver Spring, MD 20906

1. INTRODUCTION

Multi-channel remote sensing of ocean color from space has a rich history - from the past CZCS (Coastal Zone Color Scanner), to the present SeaWiFS (Sea Viewing Wide Field-Of-View Sensor), and to the near-future MODIS (Moderate Resolution Imaging SpectroRadiometer). The atmospheric correction algorithms for processing remotely sensed data from these sensors were mainly developed by Howard Gordon at University of Miami. The algorithms were primarily designed for retrieving water leaving radiances in the visible spectral region over clear deep ocean areas. The information about atmospheric aerosols is derived from channels between 0.66 and 0.87 μm, where the water leaving radiances are close to zero. The derived aerosol information is extrapolated back to the visible when retrieving water leaving radiances from remotely sensed data. For the turbid coastal environment, the water leaving radiances for channels between 0.66 and 0.87 μm may not be close to zero because of back scattering by suspended materials in the water. Under these conditions. the channels are no longer useful for deriving information on atmospheric aerosols. As a result, the algorithms developed for applications to clear ocean waters cannot be easily modified to retrieve water leaving radiances from remote sensing data acquired over the coastal environments. We have recently developed an atmospheric correction algorithm for hyperspectral remote sensing of ocean color with the near-future Coastal Ocean Imaging Spectrometer (COIS). Our algorithm uses lookup tables generated with a vector radiative transfer code developed by Ahmad and Fraser (1982) and a spectral matching technique. Channels located at wavelengths longer than 0.86 μm have been used in our derivation of information on atmospheric aerosols. The aerosol information is then extracted back to the visible based on aerosol models during our retrieval of water leaving radiances. Quite reasonable water leaving radiances have been obtained when applying our algorithm to process hyperspectral imaging data acquired over Chesapeake Bay with the Airborne Visible Infrared Imaging Spectrometer (AVIRIS), which is a good prototype for the COIS sensor.

2. BACKGROUND

Imaging spectrometry can have important applications in a variety of fields, including mineral explorations, vegetation studies, and coastal monitoring. Since mid-1980's, the concept of imaging spectrometry (Goetz et al., 1985) and hyperspectral imaging have becoming increasingly popular. In order to get useful information about earth's surface, the atmospheric absorption and scattering effects must be removed. An operational version of the atmosphere removal algorithm (ATREM) has been developed (ATREM) (Gao et al., 1993) and updated (Gao and Davis, 1997) for retrieving land surface reflectances from airborne- and spaceborne- imaging spectrometer data. ATREM has been extensively used by many investigators in different scientific disciplines as well as by university graduate students. With the experiences gained during the development of the land version of

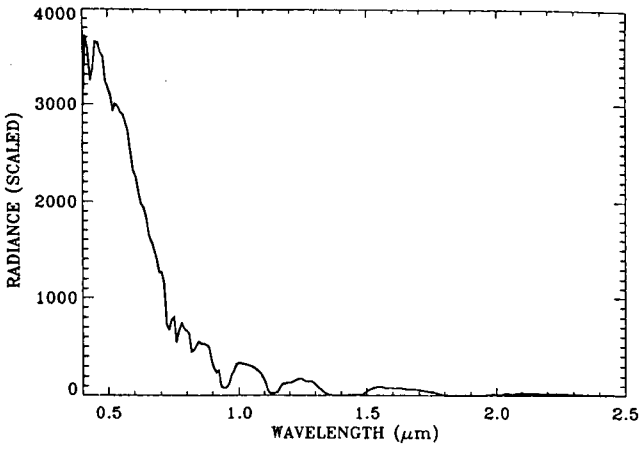

Fig. 1. An example of AVIRIS spectrum acquired over the Chesapeake Bay area in August, 1997.

ATREM code, we have developed over the past two years an operational atmospheric correction algorithm for remote sensing of ocean color from hyperspectral imaging data acquired over the coastal environment. The algorithm has been primarily developed to support the processing of spectral imaging data to be acquired with the near-future Coastal Ocean Imaging Spectrometer (COIS) (Davis and Carder, 1997) on board the Naval EarthMap Observer (NEMO) spacecraft (Wilson and Davis, 1998; Davis et al., 1998). Because the AVIRIS data acquired from an NASA ER-2 aircraft at 20 km and the near-future COIS data have similar spatial and spectral resolution and signal-to-noise ratios, we used AVIRIS data to test our algorithm during development. Figure 1 shows an example of AVIRIS spectrum acquired over the Chesapeake Bay area in August of 1997. The major atmospheric bands, such as those of water vapor centered at approximately 0.94, 1.14, 1.38, and 1.88 μm, the oxygen band at 0.76 μm, and the carbon dioxide band near 2.06 μm, are seen. An algorithm is needed to remove atmospheric absorption and scattering effects and to derive water leaving radiances (in reflectance units) from remotely sensed hyperspectral imaging data.

For the turbid coastal environment, the water leaving radiances in the 0.66 - 0.87 μm spectral region are typically not close to zero mainly because of scattering by suspended materials. Under these conditions, the channels in this spectral region have very limited use for the retrieval of information on atmospheric aerosols. Because both the algorithms of Gordon (1997) and Fraser et al. (1997) derive aerosol information from channels in the 0.66 - 0.87 μm spectral range, these algorithms cannot be easily adapted for the retrieval of water leaving radiances over coastal waters. In view of this situation, we have designed a different retrieving algorithm, which can use channels in longer wavelengths to derive aerosol information. A spectral matching technique is used in our retrievals.

3. RADIATIVE TRANSFER

For atmospheric "window" channels where the absorption by atmospheric gases is negligible, the radiance (L_{obs}) of the ocean-atmosphere system measured by a satellite instrument can be expressed as (Fraser et al., 1997),

$$L_{obs} = L_o(\lambda;\theta,\phi;\theta_o,\phi_o;\tau_a) + L_{sfc}(\lambda;\theta,\phi;\theta_o,\phi_o;W;\tau_a)\, t'_u(\lambda;\theta;\tau_a) + L_w(\lambda;\theta,\phi;\theta_o,\phi_o;W;\ \tau_a;O)\, t_u(\lambda;\theta;\tau_a), \quad (1)$$

where L_o is the atmosphere-scattered radiance, if the radiance just above the sea surface were zero; L_{sfc}

is the radiance of the light reflected from the surface; and L_w is the water-leaving radiance of light scattered from beneath the surface and penetrating it; t'_u is the upward transmittance through the atmosphere for the quantity L_{sfc}; and t_u is the upward atmospheric transmittance for the quantity L_w. L_{sfc} includes the effect of specular reflection by the air-water interfaces and the scattering effects by white caps. The independent parameters in Eq. (1) are defined as follows:

λ wavelength;

θ, ϕ view zenith and azimuth angles from a spacecraft toward earth's surface;

θ_o, ϕ_o zenith and azimuth angles of the direct sunlight;

W surface wind speed;

τ_a atmospheric aerosol optical thickness;

O norminal concentration representing combined effects from all materials beneath the air-water interface.

For convenience, we combine the first two terms in the right hand side of Eq. (1) as one term $L_{atm+sfc}$, i.e.,

$$L_{atm+sfc} = L_o(\lambda;\theta,\phi;\theta_o,\phi_o;\tau_a) + L_{sfc}(\lambda;\theta,\phi;\theta_o,\phi_o;W;\tau_a)\, t'_u(\lambda;\theta;\tau_a) \tag{2}$$

Substitute Eq. (2) into Eq. (1), we obtain,

$$L_{obs} = L_{atm+sfc} + L_w\, t_u, \tag{3}$$

We would like to follow the convention adopted in the 5S code (Tanre et al., 1990) to express radiances in reflectance units. Let's denote $\cos(\theta_o)$ as μ_o, and the downward solar irradiance at the top of the atmosphere when the solar zenith angle is equal to zero as E_o. By multiplying both sides of Eq. (3) by π and dividing them by $(\mu_o E_o)$, Eq. (3) becomes:

$$\pi L_{obs} / (\mu_o E_o) = \pi\ L_{atm+sfc} / (\mu_o E_o)\ + \pi L_w\, t_d\, t_u / (\mu_o E_o\, t_d), \tag{4}$$

where we have multiplied the numerator and denominator of the second term on the right side by the downward atmospheric transmittance t_d, which is the sum of the direct and diffuse downward transmittances of the sunlight through the atmosphere. We use several reflectances defined as

$$\rho^*_{obs} = \pi L_{obs} / (\mu_o E_o), \tag{5}$$

$$\rho^*_{atm+sfc} = \pi\ L_{atm+sfc} / (\mu_o E_o), \tag{6}$$

$$\rho_w = \pi\ L_w / (\mu_o E_o\, t_d), \tag{7}$$

where ρ^*_{obs} is the total apparent reflectance of the atmosphere-ocean system measured at the satellite level, $\rho^*_{atm+sfc}$ is the satellite level apparent reflectance resulted from the atmospheric scattering and specular reflection and white cap scattering at the air-water interface, and ρ_w is the water leaving radiance in reflectance unit, or simply the water leaving reflectance. ρ_w defined here is equivalent to the quantity $[\rho_w]_N$ defined in Eq. (2) of Gordon (1997). By substituting Eqs. (5), (6), and (7) into Eq. (4), we obtain

$$\rho^*_{obs} = \rho^*_{atm+sfc} + \rho_w t_d t_u. \quad (8)$$

In order to take account of the effect of atmospheric reflection of upward water leaving radiances back to the surface, another factor of $1 / (1 - s \rho_w)$ needs to be multiplied to the 2nd term in the right hand side of Eq. (8) (see Eqs. (11), (12), and (13) of Fraser et al. (1997)), where s is the reflectance of the atmosphere for isotropic radiance incident at its base. After inserting this factor, Eq. (8) becomes

$$\rho^*_{obs} = \rho^*_{atm+sfc} + \rho_w t_d t_u / (1 - s \rho_w). \quad (9)$$

For hyperspectral imaging data acquired from aircraft and satellite platforms and covering the 0.4 - 2.5 μm spectral region, more than half of the spectral region is affected by atmospheric gaseous absorption (Gao et al., 1993). The main contributors to the gaseous absorption are atmospheric water vapor, carbon dioxide, ozone, nitrous oxide, carbon monoxide, methane, and oxygen. We denote the total atmospheric gaseous transmittance on the Sun-surface-sensor path as T_g. We further assume that the atmospheric gaseous absorption process and the molecular and aerosol scattering process can be treated independently, i.e., we neglect the interaction term between gaseous absorption and molecular and aerosol scattering. After taking consideration of atmospheric gaseous absorption, Eq. (9) is modified as following:

$$\rho^*_{obs} = T_g [\rho^*_{atm+sfc} + \rho_w t_d t_u / (1 - s \rho_w)]. \quad (10)$$

Solving Eq. (10) for ρ_w yields

$$\rho_w = (\rho^*_{obs}/T_g - \rho^*_{atm+sfc}) / [t_d t_u + s (\rho^*_{obs}/T_g - \rho^*_{atm+sfc})]. \quad (11)$$

Given a satellite measured radiance, the water leaving reflectance can be derived according to Eqs. (5) and (11) provided that the other quantities in the right hand side of Eq. (11) can be modeled theoretically.

4. MODELING

Because of the availability of the vector radiative transfer code from Ahmad and Fraser (1982), the proper atmospheric layering structure in this code, and the treatment of wind-roughened water surfaces, we have decided to use a modified version of Ahmad and Fraser code to generate lookup tables used in our retrieving algorithm. More specifically, we use the code to generate the quantities $\rho^*_{atm+sfc}$, t_d, t_u, and s in Eq. (11). The temperature and pressure profiles assumed are the U.S. Standard Model Atmosphere (1976). No gaseous absorption is included when generating the quantities $\rho^*_{atm+sfc}$, t_d, t_u, and s, which are related to scattering by atmospheric molecules and aerosols. Four lookup tables for the quantities $\rho^*_{atm+sfc}$, t_d, t_u, and s in Eq. (11) have been generated. The values of $\rho^*_{atm+sfc}$ in our lookup table are computed for 20 aerosol models and for the following values of independent variables:

λ 0.39, 0.41, 0.44, 0.47, 0.51, 0.55, 0.61, 0.67, 0.75, 0.865, 1.04, 1.24, 1.64, 2.25 μm;

τ_a 0, 0.1, 0.2, 0.3, 0.5, 0.7, 1.0, 1.3, 1.6, and 2.0;

θ_0 1.5, 12, 24, 36, 48, 54, 60, 66, and 72 degrees;

θ 0, 1.5, 6, 12, 18, 24, 30, 36, 42, 48, 54, 60, 66, 72, 78, 84, and 88.5 degrees;

ϕ_o 0;

ϕ 0, 12, 24, 36, 48, 60, 72, 84, 90, 96, 108, 120, 132, 144, 156, 168, and 180 degrees;

W 2, 6, and 10 m/s;

O 0.

where the τ_a values are aerosol optical depths at 0.55 μm. The grids of independent variables we selected for computing are, in most cases, sufficient for interpolation later. When calculating the quantity $\rho^*_{atm+sfc}$ using the modified version of Ahmad and Fraser code, we assume that the water leaving radiance at the bottom boundary is zero, and we include the effects of specular reflection at the air-water interface and the scattering by white caps (Fraser et al., 1997). When computing the other quantities (t_d, t_u, and s), we assume that the atmosphere is bounded by a Lambertian surface with zero reflectances at the bottom boundary.

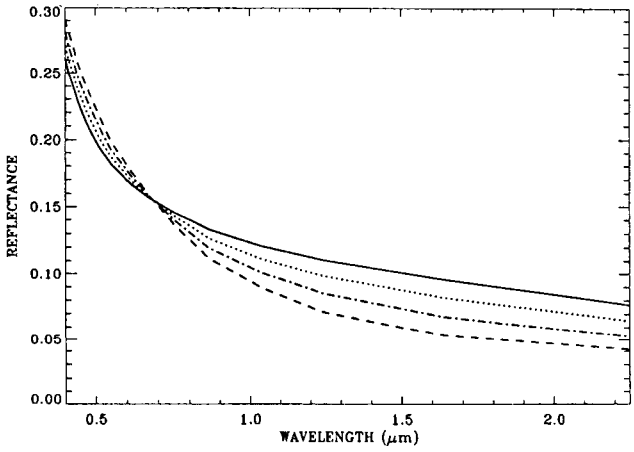

Fig. 2. Examples of simulated reflectances ($\rho^*_{atm+sfc}$) as a function of wavelength for four types of aerosol models at the same relative humidity of 50%.

Figure 2 shows examples of simulated reflectances ($\rho^*_{atm+sfc}$) as a function of wavelength for four types of aerosol models at a same relative humidity of 50% but with different particle size distributions. The simulations are made for a solar zenith angle of 36^o, a view zenith angle of 48^o, a relative azimuth angle of 156^o, an aerosol optical depth of 0.7 at 0.55 μm, and a surface wind speed of 6 m/s. The spectral slopes for the four curves change most rapidly in the 0.4 - 0.9 μm wavelength interval. This indicates that the spectra in the 0.4 - 0.9 μm region contain most of information on aerosol particle sizes. The spectral slopes for the four curves also change (though less rapidly) with wavelengths in the 1.0 - 2.25 μm region. This indicates that the spectra in the 1.0 - 2.25 μm region also contain some information about particle sizes. Therefore, it is justified to use channels in the 1.0 - 2.25 μm spectral region to estimate aerosol particle sizes from remotely sensed data acquired over coastal waters.

As shown in Fig. 1, major atmospheric absorption bands are seen in measured spectra. Typically, there are seven atmospheric gases that produce observable absorption features. These gases are: water vapor (H_2O), carbon dioxide (CO_2), ozone (O_3), nitrous oxide (N_2O), carbon monoxide

(CO), methane (CH_4), and oxygen (O_2) (Gao et al., 1993). A fast line-by-line-based module for calculating atmospheric gaseous transmittances has previously been developed in the land version of ATREM code (Gao and Davis, 1997). This module is ported over to our ocean color version of the atmosphere removal algorithm.

5. RETRIEVALS

At present, the retrievals of water leaving reflectances from measured hyperspectral imaging data cubes (two spatial dimensions and one spectral dimension) are made on a pixel-by-pixel basis. A spectral matching technique is used in the retrievals. The steps involved in the retrievals are listed below.

(a). The solar zenith and azimuth angles are derived based on the date and time of the data acquisition and on the latitude and longitude of the scene. The view zenith and azimuth angles are known.

(b). The 2-way atmospheric gaseous transmittance spectra, T_g, which match the spectral resolutions of all channels in an imaging spectrometer and correspond to the Sun-surface-sensor path, are calculated. A total of 60 transmittance spectra corresponding to vertical column water vapor amounts ranging from 0 to 15 cm are calculated. This range of column water vapor amounts covers typical atmospheric conditions in which column water vapor amounts range from about 0.4 cm to 4.3 cm. In order to get spectra corresponding to different water vapor amounts, the water vapor vertical profile is scaled by different factors during the calculations. The transmittance spectra are stored in a lookup table.

(c). A measured radiance spectrum is divided by the solar irradiance curve above the atmosphere (Neckel and Labs, 1984) to obtain the apparent reflectance spectrum (see Eq. (5)).

(d). A water vapor amount is estimated from the 0.94-μm and the 1.14-μm water vapor bands in the apparent reflectance spectrum using a 3-channel ratioing technique and a procedure to search the table containing the 60 gaseous transmittance spectra (Gao et al., 1993). Based on the estimated water vapor value and the use of the lookup table procedure again, the best estimation of gaseous transmittance spectrum corresponding to the measured spectrum is obtained.

(e). The apparent reflectance spectrum is divided by the estimated gaseous transmittance spectrum to obtain the spectrum of ρ^*_{obs}/T_g (see Eq. (11)). The values of ρ^*_{obs}/T_g corresponding to the 14 wavelengths in our tables for scattering quantities are obtained from the spectrum of ρ^*_{obs}/T_g through linear interpolation. The 14 values of ρ^*_{obs}/T_g are used in our retrieval of an aerosol model and an optical depth using a spectrum-matching technique. Figure 3a shows an example of spectrum matching using AVIRIS data on log-log plotting scales. The points derived from an AVIRIS spectrum are marked with a symbol "+" and are considered to be the "measured" data. The dotted line serves as a guide to the eye. In this case of spectral matching, the channels at 1.04, 1.24, 1.64 and 2.25 μm are assigned a weighting factor of 1, while all the other channels short of 1 μm are assigned a weighting factor of 0. The measured data for the four channels at 1.04, 1.24, 1.64 and 2.25 μm are compared with the $\rho^*_{atm+sfc}$ data stored in a pre-computed lookup table for each of the 20 aerosol models and for each of the 10 optical depths. The sum of squared differences (SSD) between the measured data and the data in the lookup table for each of the aerosol models and for each of the aerosol optical depths are calculated. The aerosol model and

Gao et al. p. 6

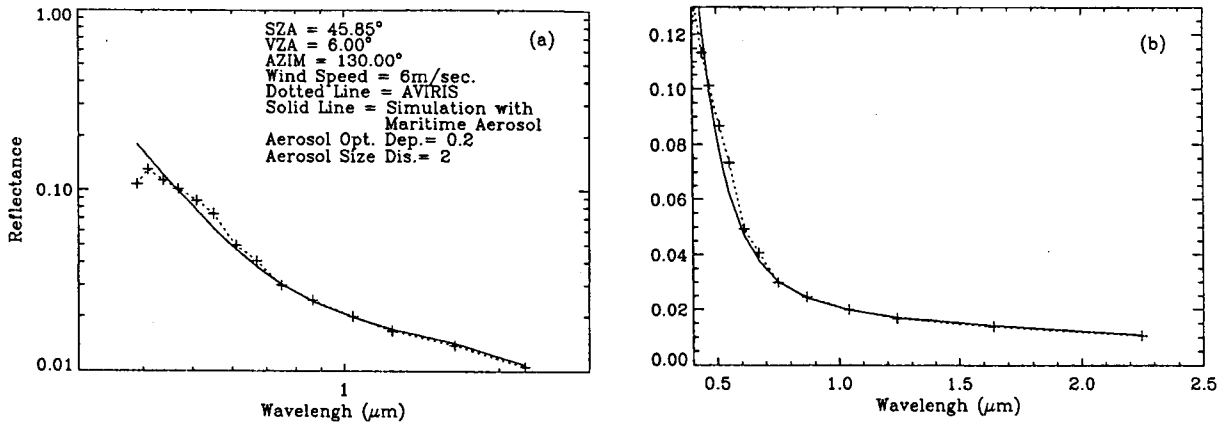

Fig. 3. (a) - an example of spectrum matching using AVIRIS data on log-log plotting scales; and (b) - same as (a), except plotted on linear-linear scales.

optical depth that give the smallest value of SSD is selected. Another aerosol model and optical depth that give the next smallest value of SSD is also selected. Based on these two aerosol models and optical depths, the final aerosol model and optical depth are determined through additional interpolating and fine fitting processes, and the values of $\rho^*_{atm+sfc}$ at the 14 wavelengths are determined. The other scattering quantities, t_d, t_u, and s (see Eq. (11)), corresponding to the selected aerosol model and optical depth at the 14 wavelengths are determined subsequently.

The solid line in Fig. 3a is the curve of $\rho^*_{atm+sfc}$ versus wavelength corresponding to our final selection of aerosol model and optical depth. The dotted curve and the solid curve agree quite well for wavelengths greater than 0.86 μm. The differences between the dotted curve and the solid curve near the 0.55 μm (green) spectral region are attributed to water leaving radiances in the visible. For wavelengths shorter than 0.45 μm, the dotted curve is below the solid curve. This is most likely due to radiometric calibration problems of AVIRIS instrument in the blue spectral region. Figure 3b is the same as Fig. 3a, except plotted on linear-linear scales.

(f). The values of the quantities $\rho^*_{atm+sfc}$, t_d, t_u, and s at the wavelength grids of an imaging spectrometer are determined through interpolations and extrapolations from the corresponding values at the 14 wavelengths determined in step (e), and the water leaving reflectance spectrum is derived according to Eq. (11).

6. SAMPLE RESULTS

The algorithm described in this paper has been applied to derive water leaving reflectances from a number of AVIRIS data sets. The retrieval results from one data set acquired over the mouth of Chesapeake Bay (37^o 12' N and 76^o 24' W) in eastern Virginia on August 17, 1997 are described below.

Figure 4a shows two radiance spectra - one measured over a very turbid area (solid line) and one over a less turbid area (dotted line) in the AVIRIS scene. Figure 4b shows the water leaving reflectance spectra retrieved from the two radiance spectra in Fig. 4a. The overall shapes of the reflectance spectra above 0.45 μm are quite consistent with those measured from other field

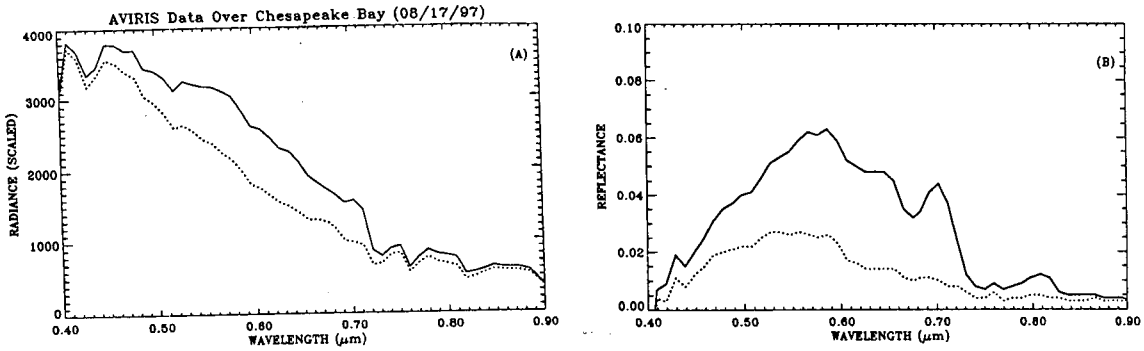

Fig. 4. (a) - AVIRIS radiance spectra measured over a very turbid area (solid line) and a less turbid area (dotted line), and (b) - the water leaving reflectance spectra retrieved from the two radiance spectra in (a).

measurements (e.g., Lee et al., 1996). Below 0.45 μm, the reflectances fall off too rapidly with decreasing wavelengths and even become negative for wavelengths less than about 0.41 μm. It is likely due to radiometric calibration of AVIRIS instrument, which reports too small radiances in the blue spectral region. We do not have field-measured reflectance spectra corresponding to the two spectra in Fig. 4b. Therefore, it is not possible in this case study to have direct comparisons between the retrieved reflectance spectra and field-measured reflectance spectra.

7. DISCUSSIONS

We have occasionally observed from other AVIRIS data sets acquired over coastal environments that the water leaving radiances for channels above 1 μm for some pixels are not close to zero; such as the situation when large amount of material is floating on the water surface. The derivation of aerosol information on aerosols from these pixels is not possible. Under this situation, we can use aerosol information derived from other pixels where the water leaving radiances above 1 μm are close to zero, and extrapolate the aerosol information to these pixels when deriving water leaving reflectances over these pixels.

8. SUMMARY

We have developed an atmospheric correction algorithm for hyperspectral remote sensing of ocean color with the near-future Coastal Ocean Imaging Spectrometer. A spectrum-matching technique is used to derive information on atmospheric aerosols. The aerosol information is extracted back to the visible based on aerosol models during our retrieval of water leaving reflectances. When using our algorithm to process hyperspectral imaging data acquired with the AVIRIS instrument over the Chesapeake Bay and Florida Keys, very reasonable water leaving reflectance spectra have been retrieved.

9. ACKNOWLEDGMENTS

The authors are grateful to Robert S. Fraser from NASA Goddard Space Flight Center (retired), Menghua Wang of University of Maryland at Baltimore County, Didier Tanre of University of Lille,

France, Yoram J. Kaufman of NASA Goddard Space Flight Center in Greenbelt, Maryland, P. Y. Deschamps of Laboratoire d'Etudes de Recherches en Teledetection Spatiale, France, Eric P. Shettle of Naval Research Laboratory in Washington, DC, and Howard Gordon of University of Miami for useful discussions during various stages of this algorithm development. The authors are also grateful to Lee F. Johnson of NASA Ames Research Center in Moffett Field, California, and to Kendall L. Carder of University of South Florida for providing some of the AVIRIS data used in this study. We gratefully acknowledge the support of the Office of Naval Research for this work.

10. REFERENCES

Ahmad, Z., and R. S. Fraser, An iterative radiative transfer code for ocean-atmosphere systems, J. Atmos. Sci., 39, 656-665, 1982.

Davis, C. O., M. Kappus, B.-C. Gao, W. P. Bissett, and W. Snyder, The Naval EarthMap Observer (NEMO) science and Naval products, Proceedings of the SPIE, v.3437, 1998.

Davis, C. O., and K. Carder, Requirements driven design of an imaging spectrometer system for characterization of the coastal environment, Proceedings of the SPIE, v. 3118, San Diego, CA, 1997.

Fraser, R. S., S. Mattoo, E.-N. Yeh, and C. R. McClain, Algorithm for atmospheric and glint corrections of satellite measurements of ocean pigment, J. Geophys. Res., 102, 17107-17118, 1997.

Gao, B.-C., K. H. Heidebrecht, and A. F. H. Goetz, Derivation of scaled surface reflectances from AVIRIS data, *Remote Sens. Env., 44*, 165-178, 1993.

Gao, B.-C., and C. O. Davis, Development of a line-by-line-based atmosphere removal algorithm for airborne and spaceborne imaging spectrometers, in *SPIE Proceedings, Vol. 3118*, 132-141, 1997.

Goetz, A. F. H., G. Vane, J. Solomon, and B. N. Rock, Imaging spectrometry for earth remote sensing, Science, 228, 1147-1153, 1985.

Gordon, H. R., Atmospheric correction of ocean color imagery in the Earth Observing system era, J. Geophys. Res., 102, 17081-17106, 1997.

Lee, Z. P., K. L. Carder, T. G. Peacock, C. O. Davis, and J. L. Mueller, Method to derive ocean absorption coefficients from remote-sensing reflectance, Appl. Opt., 35, 453-462, 1996.

Neckel, H., and D. Labs, The solar radiation between 3300 and 12500 angstrom, Solar Physics, 90, 205-258, 1984.

Tanre, D., C. Deroo, P. Duhaut, M. Herman, J. J. Morcrette, J. Perbos, and P. Y. Deschamps, Description of a computer code to simulate the satellite signal in the solar spectrum: the 5S code, Int. J. Remote Sensing, 11, 659-668, 1990.

Wilson, T., and C. O. Davis, Hyperspectral remote sensing technology (HRST) program and the Naval EarthMap Observer (NEMO) satellite, in Proceedings of the SPIE, v.3437, 1998.